

Surface treatment of electro galvanized steel in modified zinc phosphating solutions

D. I. Ivanova

University of Chemical Technology and Metallurgy, 8 "Kliment Ohridski" Blvd., 1756 Sofia, Bulgaria

Received: October 25, 2020; Revised: March 22, 2021

The effects of calcium, nickel and manganese modified zinc-phosphating baths on phosphating of electro galvanizing low-carbon steel surfaces were studied. The phosphating concentrates were characterized by their density; pH; conductivity; total and free acidity. Gravimetric, chemical, electrochemical and physical methods were used to determine the thickness, phase and chemical composition, structure, corrosion resistance and protective ability of the phosphate coatings. The results indicate that the coatings obtained with the modified solutions are thinner than the ones formed in the initial solution at the same experimental conditions: concentrations (5 %-15 % vol.) and temperatures (20°C-60°C). The phosphate coatings obtained contain mainly hopeite and the partial replacement of Zn by Ca, Ni and Mn did not affect new crystal phase formation. The corrosion resistance of the crystalline phosphate coatings was determined in model aqueous solutions of 0.01 M NaCl, 0.6 M NaCl and 0.6 M NH₄NO₃. The protective properties of the phosphate coatings were determined electrochemically by measuring the maximum anodic potential during galvanostatic polarization in a model electrolyte, as well as through neutral salt spray tests.

Keywords: zinc coatings, zinc phosphating, surface treatment.

INTRODUCTION

The production of electro galvanized steels with deposited organic (paint, polymer) coatings has been significantly increased in last years. The most important indicator of the organic coating quality is its adhesion, the main factors of which are the roughness and surface tension of the zinc surface. Therefore, the best preliminary zinc surface treatment when organic coatings are applied is the phosphating procedure that increases its roughness and surface tension about 3-4 times. The adequate phosphating and subsequent surface painting can lead to optimal corrosion protection [1].

The formation of a phosphate coating is a complex process involving subsequent dissolution of the substrate, nucleation and growth of phosphate crystals [1, 2]. The intensification of the phosphating process and the improvement of phosphate coatings deposited can be achieved by adding activators and other substances to the working solutions [3]. Commonly, addition of various metal cations such as Ca²⁺, Ni²⁺, Mn²⁺, etc. [4-7], as well as post-sealing with silicate solution [8], results in improved coating characteristics. In this context, applying the calcium-modified zinc phosphating, the presence of Ca²⁺ in the solution significantly changes the crystal structure, grain size and the corrosion resistance of the coatings [9, 10]. Otherwise, when manganese and nickel containing zinc phosphating solutions are used, the coating surface roughening decreases that results in raised corrosion resistance [11].

The phosphating of zinc surface increases its resistance several times with respect to the case of Cr⁶⁺- passivation [2]. Moreover, the phosphate coatings are more stable at high temperature in comparison with the chromate films.

The present work reports data on the phosphating process of zinc surfaces with calcium, nickel and manganese modified zinc phosphating baths. The densities, pH, conductivities, as well as the total and free acidity of the phosphating concentrates were determined. The effects of bath concentration and temperature on the coating thicknesses, structures, phase and chemical composition were studied. The corrosion resistance and the protective properties of the phosphate coatings obtained were investigated, too.

EXPERIMENTAL

Materials and samples

Disc-shaped specimens (26 mm in diameter, thickness of 1 mm and working surface area S=0.1 dm²) of low-carbon steel (0.17 % C) were coated by zinc in a conventional acid ammonium-chloride electrolyte Entobrite CLZ 953 and used for the gravimetric experiments. The electrochemical experiments were carried out with plate-shaped specimens with dimensions in accordance with ISO 17475:2005 and a fixed working surface area of 0.01 dm². In addition, square plate samples (10×10 mm) were used as specimens in all physical methods applied, while the tests of the corrosion resistance and the protective properties of the phosphate coatings on zinc surfaces were carried

* To whom all correspondence should be sent:
E-mail: dimkaivanova@uctm.edu

out with square plate coupons (50×50 mm). The thickness of the zinc coatings for all types of investigations was about 12 µm.

The preliminary treatment of the specimens prior to the phosphating included subsequent alkaline degreasing, rinsing, acid pickling, rinsing and drying [11, 14].

Solutions and working conditions

Aqueous solutions of Zn,CaPh, Zn,NiPh, and Zn,MnPh were used as working media for the crystalline phosphating depositions. They were prepared on the base of an initial ZnPh zinc phosphating concentrate through replacement of 10% of the present zinc phosphate by nickel, calcium and manganese phosphates, respectively. Thus, they were in fact concentrated solutions of the components containing acid phosphates of the corresponding metals, free phosphoric acid, inorganic salts, stabilizers, etc. The ratio $P_2O_5:NO_3^- = 1:3$ was used.

The working conditions were as follows:

- Concentration values of 5.0 vol. %, 10.0 vol. % and 15.0 vol. %;
- Temperature values of 20.0°C, 40.0°C and 60.0°C;
- Process duration of 5.0 min, 7.5 min, 10.0 min, 12.5 min and 15.0 min.

The model media used for the electrochemical characterization of the coatings were chosen in correspondence with the literature data. They were as follows: 0.01 M NaCl, 0.6 M NaCl, and 0.6 M NH_4NO_3 [13].

The protective properties of the phosphate coatings were determined in a model ($NaCl + Na_2SO_4$; 6 g l^{-1} + 94 g l^{-1}) electrolyte [15].

Methods of investigation

Gravimetric method. The method was used to investigate the influence of various factors on the kinetics of phosphate coatings formation. Its application requires careful determination of the samples mass (in grams) after phosphatizing (m_1), as well as their mass after the coating removal (m_2). Using the following equation allows determination of the phosphate coating thickness, M [11]:

$$M = \frac{(m_1 - m_2)}{S}, g m^{-2},$$

where, S - sample surface area, m².

Open circuit potential determination. Metals or metal-coated substrates immersed in liquid electrolyte media resulted in establishment of non-equilibrium, i.e. the so-called corrosion potentials. The corrosion potentials are not indicative with respect to the resistance attained but their values and time variations provide enough information about

the character of the corrosion process, the behavior of both the metal and metal coating in different media under various conditions. The experiments were performed with an automatic device EG&G Princeton Applied Research, potentiostat/galvanostat, model 263A.

Potentiodynamic polarization method. The polarization curves recorded potentiostatically or potentiodynamically allow determination of various corrosion characteristics such as E_{corr} , i_{corr} , etc. The cell employed was a three-electrode one with compartments for the test electrode (0.11), the counter Pt-electrode (0.2 cm²) and the saturated calomel reference electrode (SCE). The experiments were carried out with EG&G Princeton Applied Research potentiostat/galvanostat, model 263A, provided with the specialized software package PowerCORR[®].

Scanning electron microscopy (SEM). This is the most widely used method of surface topography investigation. The analyses were put through a scanning electron microscope JEOL JSM 6390 equipped with a scanning system of ultra-high resolution (ASID-3D).

Energy-dispersive spectroscopy (EDS). This local X-ray spectral investigation method providing qualitative and quantitative analysis of the composition of surface microvolumes of the order of several µm³ was carried out by the scanning electron microscope JEOL JSM 6390 equipped for EDS.

X-ray photoelectronic spectroscopy (XPS). The method allows direct investigation of the electrons situated in the valence, as well as in the inner electron layers. The measurements were carried out with the Escalab II system equipped with an X-ray source of AlK_{α} (1486.6 eV) and a maximum instrumental resolution of 1 eV.

X-ray phase analysis (XRD). The method allows quantitative determination of the phases in the system (of 1 % – 3 % content), their chemical composition, the structure of the phase unit cell, etc. Philips APD-15 (1030) X-ray diffractometer equipped with Bragg-Brentano focusing system was used.

Atomic force microscopy (AFM). The method allows determination of the surface topography through a direct contact with a probe fixed at the end of the microscopic beam. The measurements were carried out with the Nano Scope V system (Veeco Instruments Inc.). The data obtained were treated by WSxM5.0 Develop 3.0 Software.

Electrochemical determination of the protective properties of the specimens. The method uses measurements of the maximum anodic potential, E_{Amax} under galvanostatic polarization in a model

electrolyte solution ($\text{NaCl} + \text{Na}_2\text{SO}_4$; $6 \text{ g l}^{-1} + 94 \text{ g l}^{-1}$) with the assumption that higher values of E_{Amax} correspond to better corrosion resistances [16]. Corrosion tester characterized the anodic behavior of the coatings. The time variations of the anodic potentials were recorded by EG&G Princeton Applied Research potentiostat/galvanostat, model 263A and treated by the corrosion software Softcorr II.

Neutral salt spray (NSS) corrosion investigations. The NSS corrosion tests were carried out in accordance with ISO 9227:2012 recommendations. The test carried out in an NSS chamber included 4 cycles lasting 24 hours each, i.e. totally 96 hours. The corrosion resistance (the coating corrosion in this case) and the corrosion protection ability (i.e. the steel substrate corrosion) were evaluated after each cycle. Such corrosion studies could be extended up to 8 cycles in order to evaluate the corrosion behavior of each series of coating tests. NSS chamber commercially provided by VSN 1000 Heraeus-Vötsch GmbH was used.

RESULTS AND DISCUSSION

The data summarized in Table 1 show the most important indicators characterizing the phosphating concentrates used in the experiments: density, ρ ; pH; conductivity, σ ; total, K_{ta} , and free, K_{fa} , acidity. The data indicate that the densities of all concentrates are almost identical.

Table 1. Phosphating concentrate characteristics

Solution	ρ , g cm^{-3}	pH	σ , mS cm^{-1}	K_{TA}	K_{FA}
ZnPh	1.330	0.32	110.7	304	35
Zn,CaPh	1.320	0.31	110.5	304	40
Zn,NiPh	1.330	0.41	105.4	302	33
Zn,MnPh	1.325	0.21	113.2	304	44

In the case of Zn,NiPh, the phosphating concentrate containing Ni has the lowest conductivity and the highest pH, while Zn,MnPh modified by Mn has the lowest pH. The solution K_{TA} values differ insignificantly, while K_{FA} is higher in cases of Zn,CaPh and Zn,MnPh. The greater difference in some of the characteristics of the phosphating concentrates studied can be attributed only to the nature and properties of the various cations used for modification of the initial zinc-containing concentrate ZnPh.

Gravimetric investigations

The method was used to elucidate the effect of the operating conditions (concentration and temperature of the phosphating solutions, as well as duration of the process) on the coating thickness M . The values of the concentration and temperature are selected experimentally. Figures 1, 2, 3 and 4 indicate typical thickness/mass, M vs. time, τ relationships of the coatings obtained in solutions of different concentrations at different temperature values.

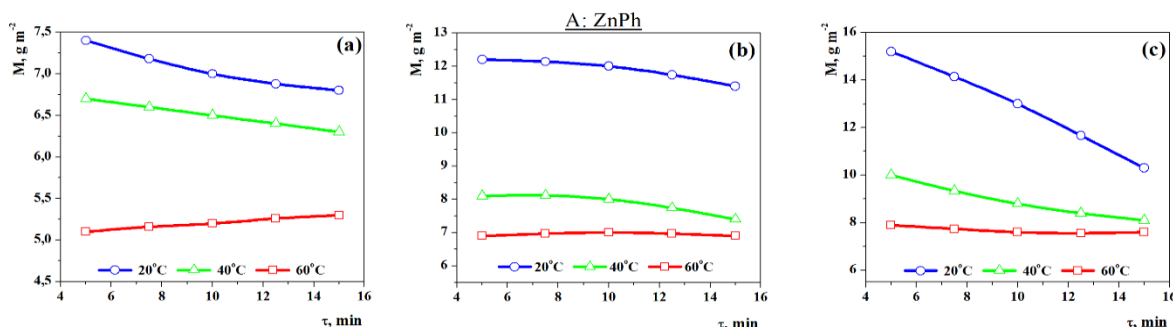


Figure 1. Effect of the phosphating duration, τ , on the thickness/mass of the phosphate coating obtained, M : a – 5 %; b – 10 %; c – 15 % (A: ZnPh)

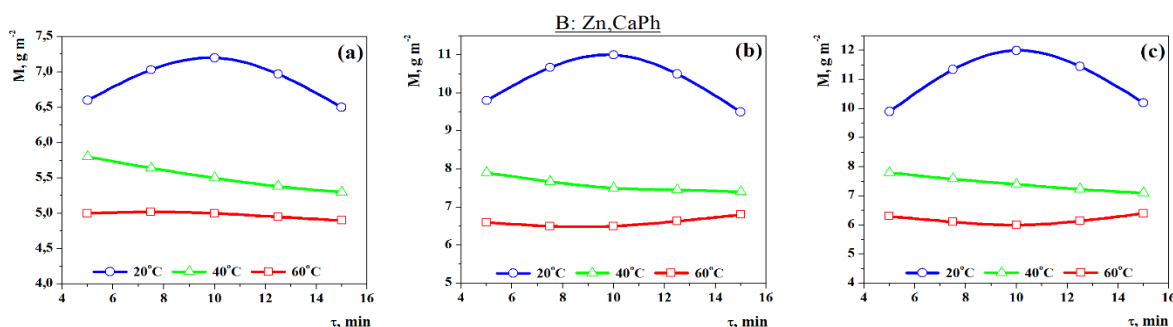


Figure 2. Effect of the phosphating duration, τ , on the thickness/mass of the phosphate coating obtained, M : a – 5 %; b – 10 %; c – 15 % (B: Zn,CaPh)

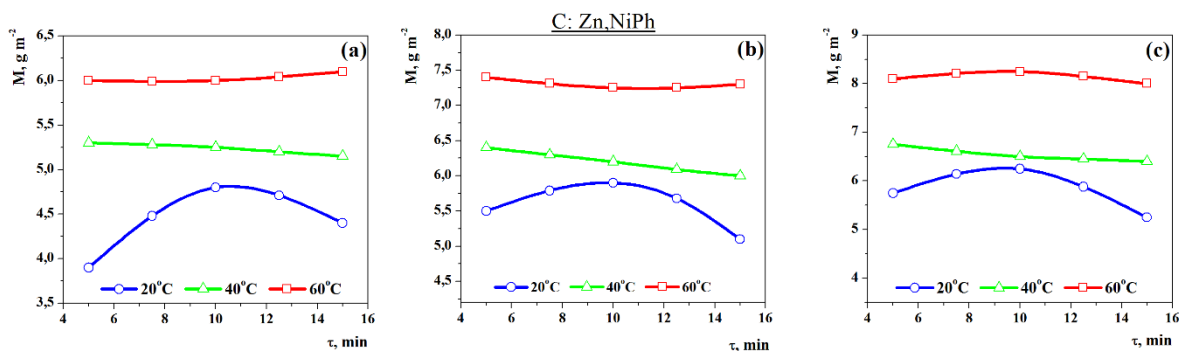


Figure 3. Effect of the phosphating duration, τ , on the thickness/mass of the phosphate coating obtained, M : a – 5 %; b – 10 %; c – 15 % (C: Zn,NiPh)

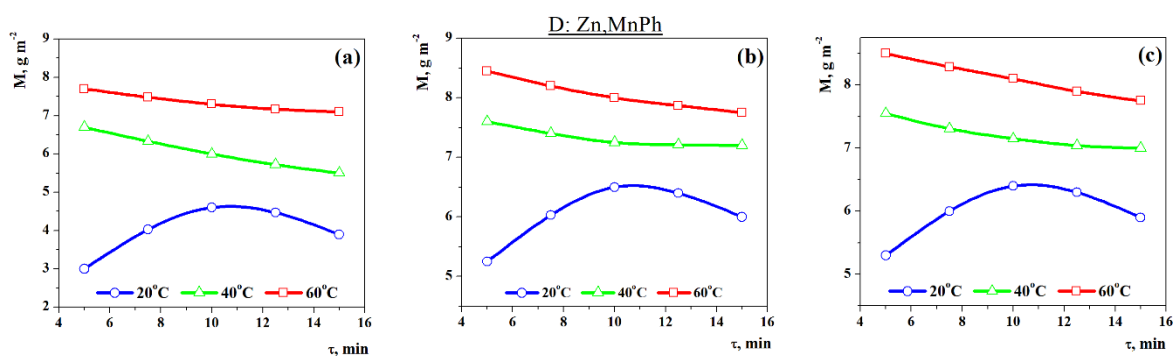


Figure 4. Effect of the phosphating duration, τ , on the thickness/mass of the phosphate coating obtained, M : a – 5 %; b – 10 %; c – 15 % (D: Zn,MnPh)

The shapes of the curves in Figures 1 and 2 indicate that the coatings of highest thickness correspond to the shortest time runs of 5 min in ZnPh and Zn,CaPh irrespective of the concentration and the temperature of the working solutions. The thickness of the coating decreases or stays relatively unchanged at longer duration. These facts suggest that the phosphate coatings on the zinc surfaces are growing with the highest rate in the initial stage (up to 5 min). Then their reorganization proceeds – exchange with the solution’s components resulting in increase of their density, homogenization and mass decrease. An exception was observed in the thickness (M) variation when the specimens were treated at 20°C in Zn,CaPh solutions irrespective of the variations in the concentration (Figure 2). In this case, the top values of M were reached in the first 10 minutes of the phosphating process. This is most probably due to the effect of the calcium cations on the processes of crystal nuclei formation and the consequent growth of the crystals in the course of phosphatizing, owing to the variations in their rates mainly at low temperatures [17].

Figures 1 and 2 also show that the thickness of the coatings increases with the concentration rise in both solutions studied. It is highest at 20°C and

lowest at 60°C. The presence of calcium cations in the phosphating bath Zn,CaPh results in a decrease of the coatings thickness under all experimental conditions considered when compared to the changes observed in the initial zinc phosphating solution. The visual observations ($\times 10$) of the phosphated zinc surfaces indicate that the homogeneity and the density of the coatings obtained in both solutions increase with increase in the temperature.

The modification of ZnPh by nickel and manganese cations, Zn,NiPh and Zn,MnPh, brings about essential variations of the thickness, M vs. time, τ dependences (see Figures 3 and 4). In this case, the crystalline phosphate coatings of the highest thickness were obtained in the first 5 min of the process, in both solutions at the highest temperature value studied, i.e. at 60°C. The lowest thicknesses were obtained at the temperature of 20°C. The thicknesses of the coatings obtained at 40°C and 60°C decreased gradually with the increase in the phosphatizing duration and the effect could be most probably attributed to the coating reorganization taking place. At the lowest temperature of the solution (20°C), the thickest coatings were obtained up to the 10th min of the phosphatizing process.

Electrode potential measurements

The electrode potentials of the phosphated steel specimens were measured in the course of the crystalline coatings formation in the corresponding phosphating baths and at their testing in model aqueous media. The change in the potential in the course of phosphating is related to the nature and the homogeneity of the coating obtained, whereas the stabilization of the electrode potentials indicates in fact the end of the phosphating procedure. The time-variation of the electrode potentials in the course of the phosphate coatings growth is shown in Figure 5.

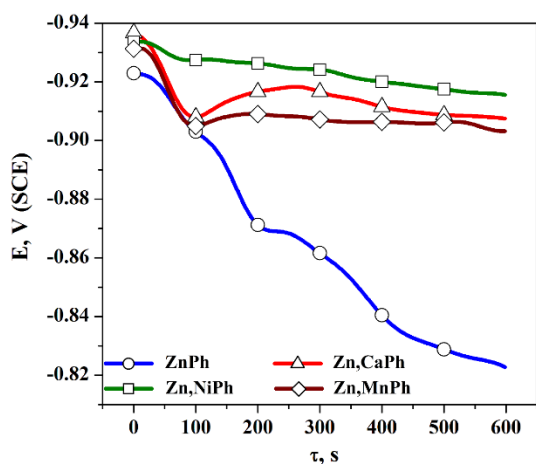


Figure 5. Potential vs. time relationships recorded in the course of crystalline phosphate coatings formation: 10 vol.%, 60°C, 10 min.

The potential, E vs. time, τ relationships were recorded under identical experimental conditions, that is: working solution concentration of 10 vol.%, temperature of 60°C and duration of 10 min. The shape of the curves indicates that within the initial short period (20 – 25 s) constant potentials were observed and followed by their shift in a positive direction. This is most clearly demonstrated by the

results obtained with the ZnPh solutions containing only zinc phosphate, while in the modified phosphating solutions it is more slightly expressive and is in the following order: $E_{Zn,NiPh} < E_{Zn,CaPh} < E_{Zn,MnPh}$. The course of the curves allows suggesting that the nuclei formation, the consequent growth and density of the coatings are stimulated in the modified phosphating solutions.

The corrosion resistance, i.e. the respective protective ability of the crystalline phosphate coatings was determined in model aqueous solutions of 0.01 M NaCl, 0.6 M NaCl and 0.6 M NH_4NO_3 . The experiment itself refers to dipping of the phosphated specimens in the solutions studied. The coatings are determined to be corrosion resistant if no changes on the specimens' surface or model solution coloring are observed within one hour after the dipping. The tests carried out indicate that there are no changes in all phosphate coatings and they are determined as highly resistant against corrosion in these media.

The corrosion potentials of the phosphated specimens in the model media were determined and compared to those corresponding to cold galvanized steel surfaces (without phosphate coatings). The potentials of the crystalline phosphate coatings in both NaCl media are shown in Figure 6 (a) and (b). In this case, the potentials shift to more negative values and after some period remain almost constant. The potentials of the non-phosphated zinc specimens attain intermediate values but they are more negative than the potentials of the specimens treated in the nickel-modified and the initial (non-modified) zinc phosphating solutions. The potentials of the specimens treated in calcium and manganese modified solutions attain more positive values. The results allow classifying the phosphate coatings with respect to their protective abilities although the differences in the potential values are relatively small.

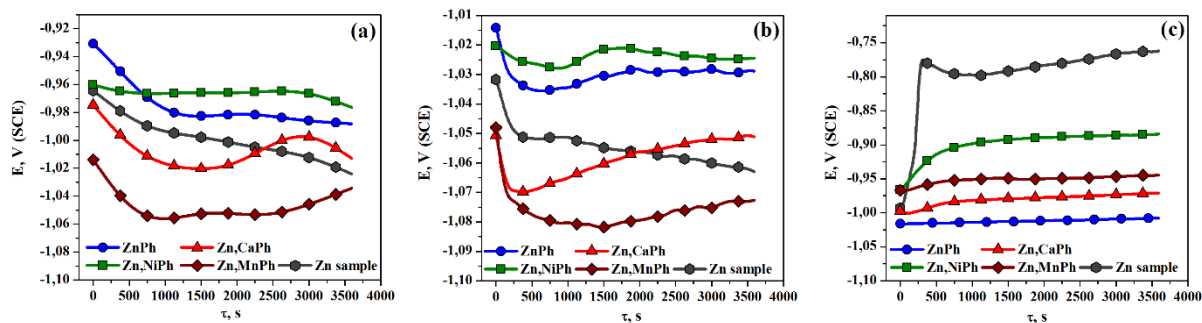


Figure 6. Potential vs. time (E- τ) dependence of phosphate coatings recorded at 20°C in: a – 0.01 M NaCl; b – 0.6 M NaCl; c – 0.6 M NH_4NO_3

The electrode potentials variations obtained in 0.6 M NH_4NO_3 solution are shown in Figure 6 (c).

The initial slight shift in a positive direction is followed by a certain period where the values of the

potentials remain almost constant. The coatings formed in ZnPh solutions exhibited the most negative potentials, followed by those formed in ZnCaPh, Zn,MnPh and Zn,NiPh solutions – the potentials gradually shifted in a positive direction. The curve demonstrating the time-variation of potential of non-phosphated zinc surface within the first 200-250 s indicates an average shift of about 250 mV in a positive direction. This shift, which is essentially greater than that in the cases with phosphated surfaces, is followed by a period where the potential remains almost without alteration.

Potentiodynamic polarization investigations

The potentiodynamic polarization studies of the crystalline phosphate coatings were carried out at 20°C in model aqueous solutions of 0.01 M NaCl, 0.6 M NaCl and 0.6 M NH₄NO₃.

The scanning rate of 10 mV s⁻¹ was chosen based on preliminary test runs. The target of these experiments was to obtain information about the corrosion behavior of the crystalline phosphate coatings formed in the corresponding model media in the course of their cathodic and anodic polarization and consequently to compare them.

The potentiodynamic polarization relationships of the phosphate coatings (Figure 7) obtained in the model solutions of NaCl and NH₄NO₃ allow estimating both the corrosion potentials and the corresponding corrosion currents summarized in Table 2. The modifications of the zinc phosphate baths by nickel, calcium and manganese result in shifts of the coating potentials of about 25 mV-100 mV in a positive direction in both NaCl solutions tested. This effect is not so well demonstrated when solutions with higher sodium chloride concentrations were used. The more positive potentials of the modified phosphate coatings indicate higher corrosion resistances and improved protective abilities when they are compared to the reference zinc surfaces despite the fact that the corrosion currents slightly differ.

The corrosion potentials and the corresponding currents related to the crystalline phosphate coatings developed in 0.6 M NH₄NO₃ solutions are also summarized in Table 2. These corrosion potentials are more positive while the corrosion currents are higher with respect to those determined in NaCl solutions.

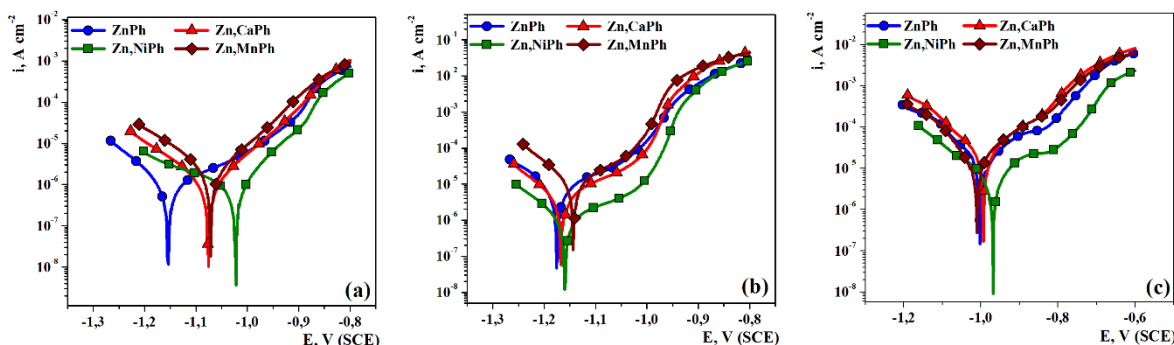


Figure 7. Potentiodynamic polarization relationships of crystalline phosphate coatings at 20°C in: a – 0.01 M NaCl; b – 0.6 M NaCl; c – 0.6 M NH₄NO₃

Table 2. Corrosion current and potential values

Model medium	ZnPh		Zn,CaPh		Zn,NiPh		Zn,MnPh	
	E _{corr} , mV	i _{corr} , A cm ⁻²	E _{corr} , mV	i _{corr} , A cm ⁻²	E _{corr} , mV	i _{corr} , A cm ⁻²	E _{corr} , mV	i _{corr} , A cm ⁻²
0.01 M NaCl	-1154	7.1×10 ⁻⁷	-1076	8.2×10 ⁻⁷	-1022	8.6×10 ⁻⁷	-1072	9.1×10 ⁻⁷
0.6 M NaCl	-1175	4.6×10 ⁻⁶	-1168	4.1×10 ⁻⁶	-1159	2.4×10 ⁻⁶	-1143	6.4×10 ⁻⁶
0.6 M NH ₄ NO ₃	-1051	6.4×10 ⁻⁵	-1035	3.2×10 ⁻⁵	-986	1.6×10 ⁻⁵	-1022	4.2×10 ⁻⁵

SEM analysis

The microphotographs (SEM) of the phosphate coatings obtained on electrogalvanized steel in ZnPh, Zn,CaPh, Zn,NiPh and Zn,MnPh, developed for 10 min at 60°C in a solution of 10 vol. % concentration, reveal that the habitus of the coatings is almost the same (Figure 8). Precisely, the crystals are formed at a single center with a growing mode similar to that of spherulites. The crystal dimensions are within the range of 2 µm-200 µm. There are relatively well-displayed differences that could be attributed to the presence of some better and greater leaf-like crystals grown in Zn,NiPh and Zn,MnPh.

EDX analysis

The quantities of the main elements found in the coatings obtained for 10 min at 60°C in solutions of a concentration of 10 vol.% are summarized in Table 3. The EDX data indicate almost identical amounts of O, P and Zn in all coatings tested. Presence of Ca, Ni and Mn was not detected in the composition of the coating grown in ZnPh solutions but quantities of these elements were discovered in the coatings formed in the modified zinc-phosphating baths.

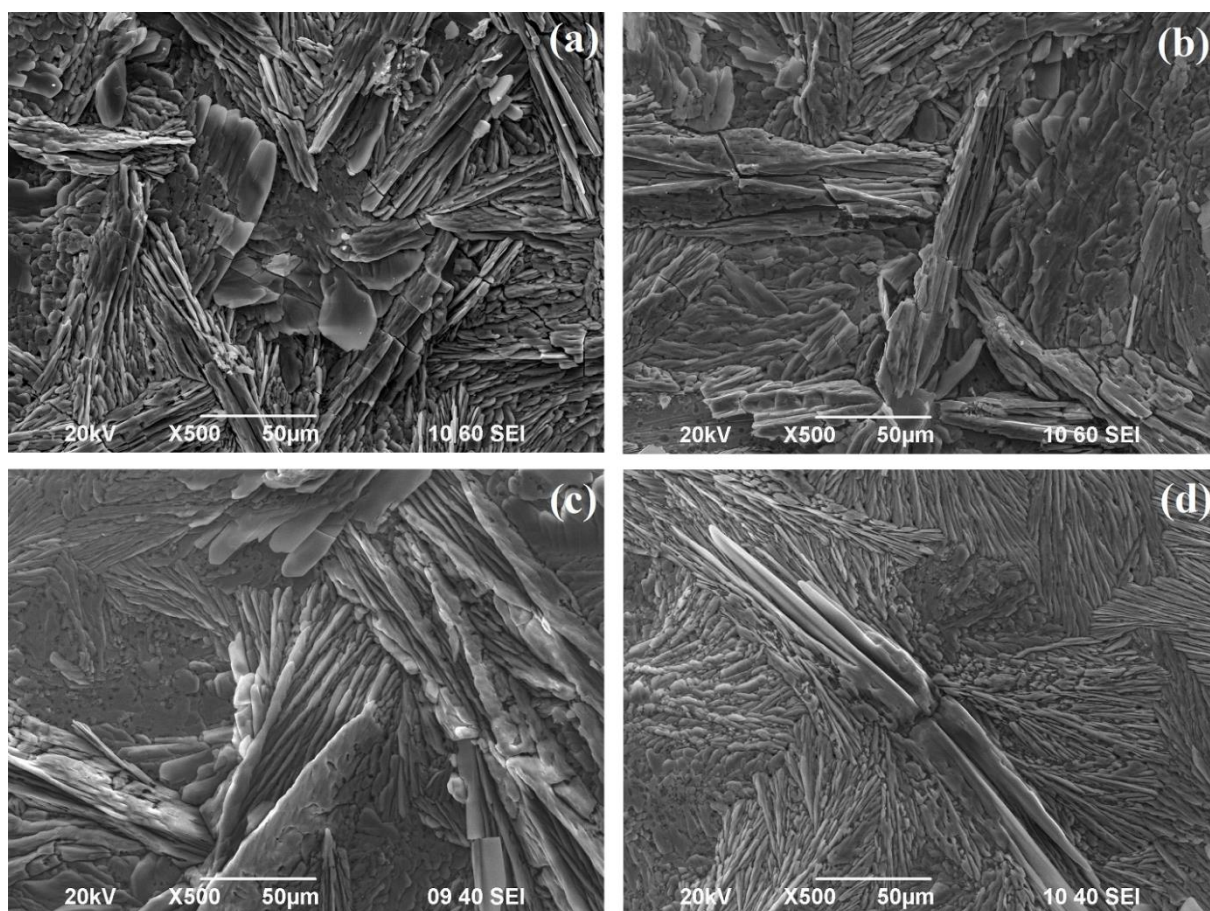


Figure 8. Microphotographs of phosphate coatings grown in: a – ZnPh; b – Zn,CaPh; c – Zn,NiPh; d – Zn,MnPh

Table 3. Elemental composition of the phosphate coatings obtained by EDX – analysis

Elements	ZnPh		Zn,CaPh		Zn,NiPh		Zn,MnPh	
	Wt %	At %	Wt %	At %	Wt %	At %	Wt %	At %
O	43.24	70.96	37.90	67.00	37.94	64.26	35.40	65.13
P	13.99	11.86	12.60	11.51	11.85	0.37	11.43	10.86
Zn	42.76	17.18	48.38	20.93	46.39	19.23	52.50	23.65
Ni	-	-	-	-	3.82	6.14	-	-
Ca	-	-	1.12	0.56	-	-	-	-
Mn	-	-	-	-	-	-	0.67	0.36
Total	100	100	100	100	100	100	100	100

XRD analysis

The XRD spectra of the crystalline coatings grown in the initial and the modified phosphating solutions are shown in Figure 9. The XRD analysis principally indicates the presence of hopeite – $Zn_3(PO_4)_2 \cdot 4H_2O$ in the coatings. There are shifts of some of the peaks in the spectra corresponding to coatings obtained in the modified solutions, as well as changes in their intensities when compared to the data obtained with coatings formed in the initial zinc-containing solution. These shifts suggest partial displacement of Zn in the hopeite by Ca, Ni and Mn but this does not lead to appearance of new phases. In fact, quasi-hopeites of calcium, nickel and manganese, are formed.

X-ray photoelectron spectroscopy (XPS)

The X-ray photoelectron spectroscopy was applied to determine both the nature and the valent state of the elements present on the coatings surfaces. The peaks observed refer to Zn2p, O1s, P2p and Fe2p as it is shown in Figure 10. The binding energies of Zn2p and O1s were estimated as 1021.6 eV and 532.0 eV, respectively and

corresponded to ZnO. The estimated binding energy of P2p was about 134.2 eV. This suggests that the element existing in its V-valent state is incorporated in a compound of the form of P_2O_5/PO_4^{-3} . The Fe2p peak was found in the spectra of all crystalline phosphate coatings. The presence of small quantities of iron (see Table 4) could be attributed to the zinc coating of the sample substrate. The peaks corresponding to Ca2p, Ni2p and Mn2p peaks are shown in Figure 11. Precisely, they were detected in the photoelectron spectra of the coatings developed in the modified phosphating solutions. The values of the binding energies are as follows: 348.2 eV for Ca2p, 855.0 eV and 861.2 eV for Ni2p, and 642.4 eV for Mn2p. These values suggest that the coatings are mainly in the form of oxides and the calcium and nickel cations are in their second-valent states, while the manganese cations are in their fourth-valent state.

The concentration values corresponding to the elemental analysis of the different phosphate coatings obtained by XPS analysis are summarized in Table 4.

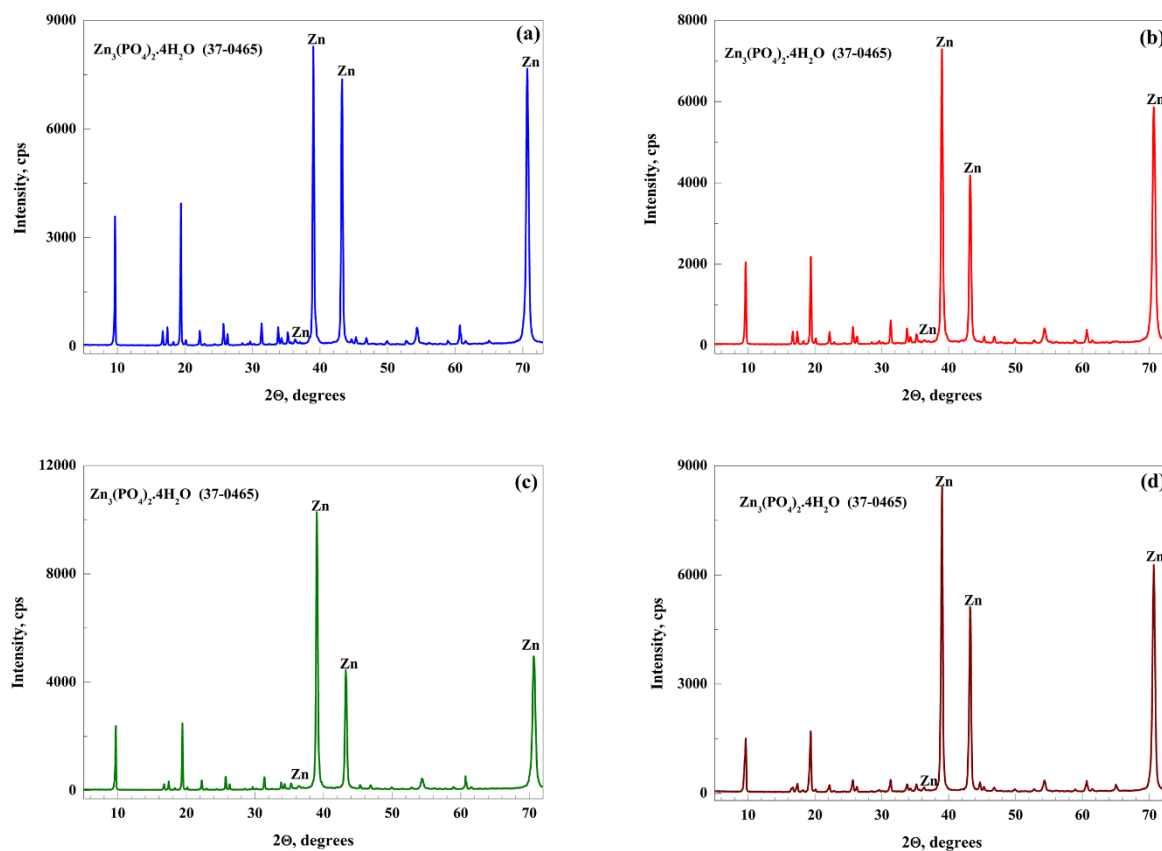


Figure 9. XRD spectra of the crystalline phosphate coatings grown in: a – ZnPh; b – Zn,CaPh; c – Zn,NiPh; d – Zn,MnPh

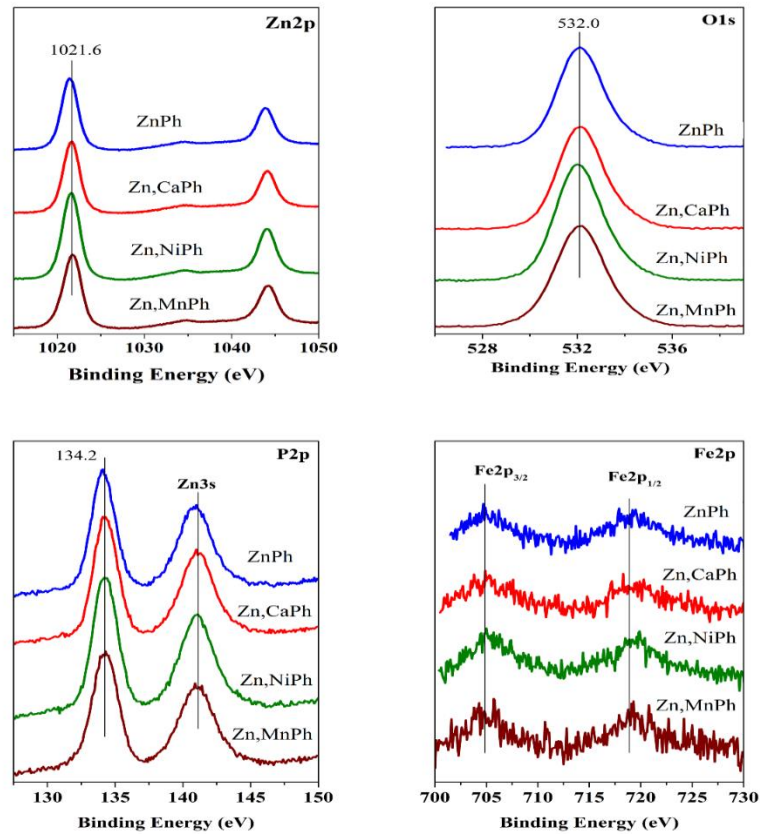


Figure 10. XPS spectra of the crystalline phosphate coatings illustrating the presence of Zn2p, O1s, P2p and Fe2p peaks.

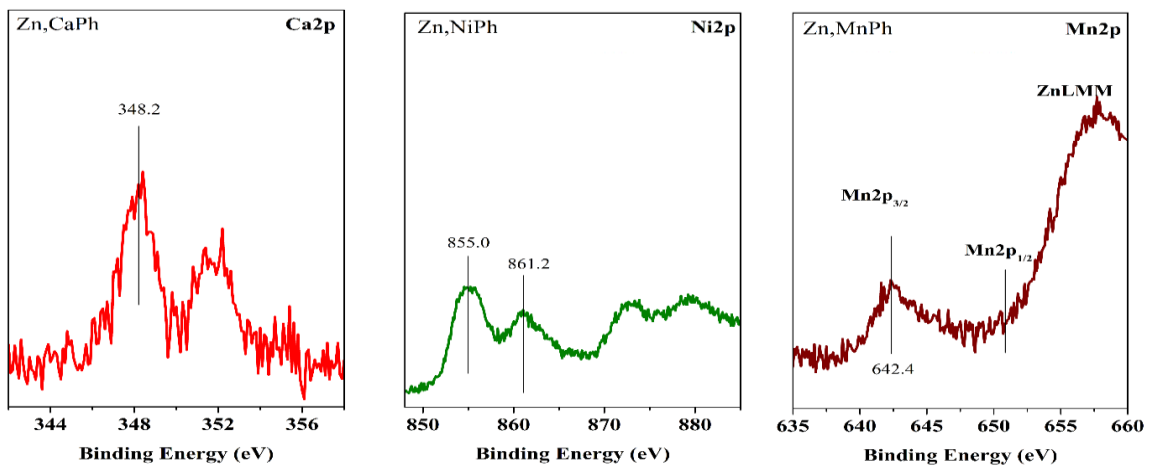


Figure 11. XPS spectra illustrating the presence of Ca2p, Ni2p and Mn2p peaks in the coatings grown in: a – Zn,CaPh; b – Zn,NiPh; c – Zn,MnPh

Table 4. Elemental composition of the phosphate coatings obtained by XPS – analysis

Elements	ZnPh	Zn,CaPh	Zn,NiPh	Zn,MnPh
	At %	At %	At %	At %
O	64.9	65.0	64.0	64.4
P	20.1	19.4	19.3	18.9
Zn	14.6	13.6	14.8	14.6
Fe	0.4	1.0	0.7	0.9
Mn	–	–	–	1.2
Ni	–	–	1.2	–
Ca	–	1.0	–	–

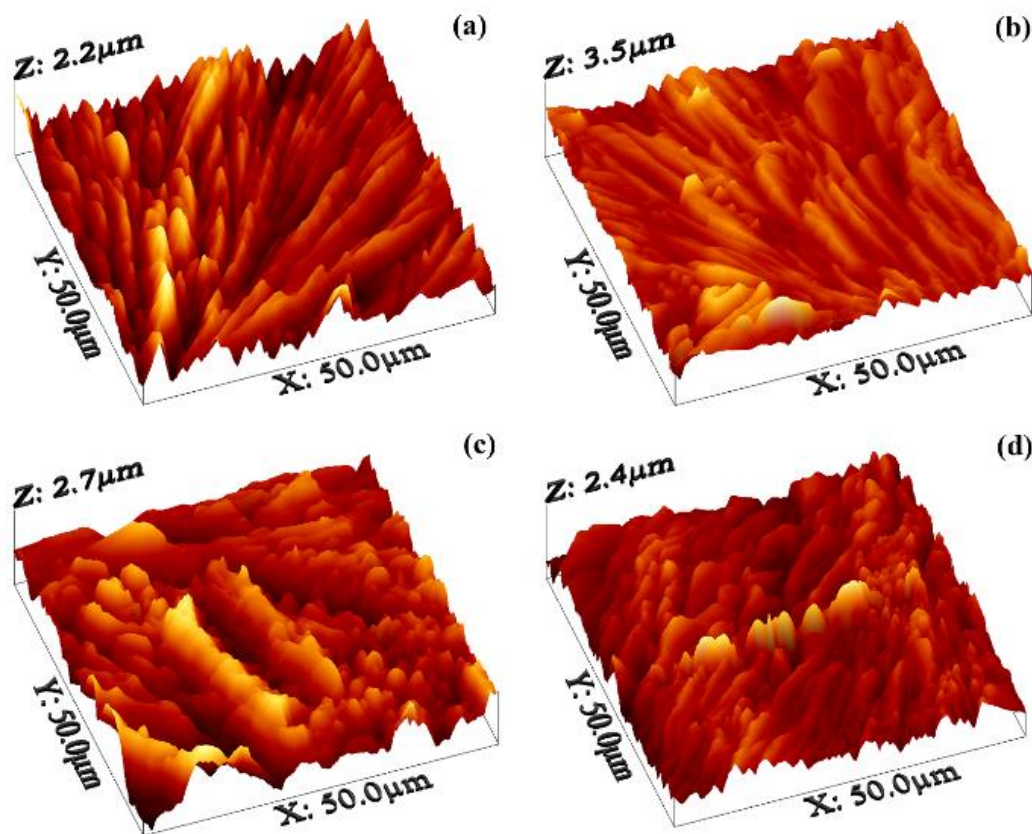


Figure 12. AFM three-dimensional images of the surface of the crystalline phosphate coatings grown in: a – ZnPh; b – Zn,CaPh; c – Zn,NiPh; d – Zn,MnPh

Atomic force microscopy (AFM) data

The three-dimensional contour maps determined by AFM (see Figure 12) indicate well-developed crystalline structures of the coatings. The latter determined the dimensions ($50\mu\text{m} \times 50\mu\text{m}$) of the scanned area used for the analysis.

Electrochemical determination of the phosphate coatings protective properties

The electrochemical determination of the protective properties of phosphate coatings consist in measuring the maxima of the anodic corrosion potential, E_{Amax} during galvanostatic polarization in a model electrolyte ($\text{NaCl} + \text{Na}_2\text{SO}_4$; $6 \text{ gl}^{-1} + 94 \text{ gl}^{-1}$). Three samples from each series of specimens with identical coatings were tested aiming higher precision and at least three replicates were measured of each sample. Some of the profiles of the polarization potentials against time are shown in Figure 13.

The better corrosion protective properties correspond to the higher E_{Amax} and to the bigger integral area under the maxima. The data presented show that close values of E_{Amax} correspond to coatings formed in ZnPh and Zn,CaPh.

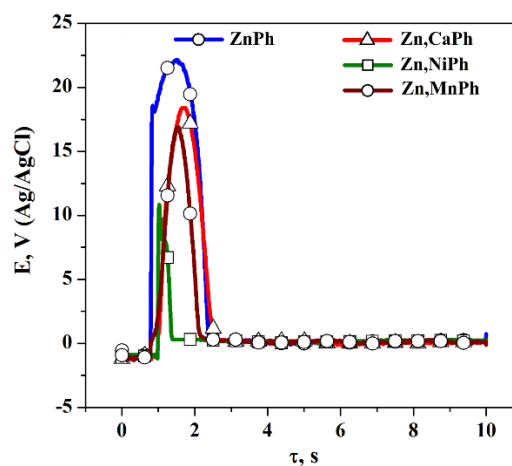


Figure 13. Potential vs. time ($E, V - \tau, s$) dependences of the crystalline coatings obtained during galvanostatic polarization.

Corrosion tests in a neutral salt spray (NSS)

The NSS corrosion tests were carried out in accordance with the procedure described in ISO 9227:2012. The initial visual observations of the specimens indicated acceptable homogeneities of the surfaces. The corrosion tests addressed one side of the samples, while the opposite ones were used for electrochemical experiments. Three specimens of each coating series were examined.

A. Corrosion resistance of the coatings. Essential changes in the outer appearances of all specimens were observed immediately after the first cycle. Precisely, the samples became covered to varying extents by white corrosion products (*white rust*) indicating the zinc corrosion in NSS. The most aggressive white rust appeared when samples with zinc coating only were tested, which is an expected result.

B. Corrosion protection provided by the coatings investigated. Specimens of all series (including three with a zinc coating only) do not corrode until the appearance of *red rust* formation (0% affected area) irrespective of the significant corrosive impact of the *white rust* on some of the series. Examination marks of 10 were assigned to these samples, evaluating in this way their corrosion resistances in comparison with the steel substrate until the end of the corrosion tests (the end of the 8-th corrosion cycle).

The experiments with phosphated coatings developed in different native and modified solutions allowed to outline the main results among them: the tests indicated that all samples became covered by white rust after the first corrosion cycle. This effect was stronger with specimens with no phosphate coatings while the samples with phosphate coatings (of the 5-th÷8-th series) were almost identically affected by white rust on both sides of the plates. The latter can be attributed to the fact that the crystalline phosphate coatings do not participate alone in the corrosion test but as layers attached to sublayers better adhere to the substrates.

The tests with almost all crystalline phosphate coatings revealed that corrosion products formed on the surfaces after the first run remained practically unchanged until the end of the experiments. No red rust appeared on the specimens of all series until the end of the 8-th cycle.

The results related to the corrosion behavior in a neutral salt spray and the electrochemical experiments demonstrate satisfactory correlations and interrelations, which allows obtaining reliable characteristics of the phosphate coatings investigated.

CONCLUSIONS

On investigating the phosphating of electro galvanized low carbon steel surfaces in calcium, nickel and manganese modified zinc-phosphating baths (ZnPh), it was established that:

The phosphating in Zn,NiPh and Zn,MnPh, as well as in Zn,CaPh leads to the formation of thinner coatings under all experimental conditions investigated when compared to those grown in the zinc phosphating bath – ZnPh.

The modification of the zinc phosphate bath by calcium, nickel and manganese results in shifts of the coating potentials of about 25 mV-100 mV in a positive direction in all tested media.

The crystals of the coatings are formed at a single center with a growing mode similar to that of spherulite. The crystal dimensions are within the range of 2 µm-200 µm.

The EDX data indicate almost identical amounts of O, P and Zn in all coatings tested. Presence of Ca, Ni and Mn was not detected in the composition of the coating grown in ZnPh solutions.

The X-ray phase analysis showed the presence of mainly hopeite – $Zn_3(PO_4)_2 \cdot 4H_2O$ in the phosphate coatings. Weak removing to some of the diffraction pattern peaks was observed. The latter is probably due to partial replacement of the zinc in hopeite by calcium, nickel and manganese, but it is not sufficient to clearly characterize the differentiation of new phases.

The protective properties of the phosphate coatings were determined electrochemically by measuring the maximum anodic potential, $E_{A,max}$ during galvanostatic polarization in a model (NaCl + Na₂SO₄; 6 g l⁻¹ + 94 g l⁻¹) electrolyte, as well as through neutral salt spray tests.

REFERENCES

1. D. Rausch, The Phosphating of Metals, Finishing Publications Ltd, Teddington, Middlesex, England, 1990, pp. 47, 151.
2. D. B. Freeman, Phosphating and Metal Pretreatment, Woodhead-Foulkner, Cambridge, 1986, pp. 9, 118.
3. Zh. Gao, D. Zhang, X. Li, Sh. Jiang, Q. Zhang, *Colloids and Surfaces A: Physicochemical and Engineering Aspects*, **546**, 221 (2018).
4. J. Donofrio, *Metal Finishing*, **98** (6) 57, 60 (2000).
5. U. B. Nair, *Metal Finishing*, **93**, 40 (1995).
6. A. S. Akhtar, D. Susac, P. Glaze, K. C. Wong, P. C. Wong, K. A. Mitchell, *Surf. and Coat. Tech.*, **187**, 208 (2004).
7. M. Tamilselvi, P. Kamaraj, M. Arthanareeswari, S. Devikala, J. Arockia Selvi, *Intern. J. of Adv. Chem. Sci. and Applications*, **3** (1), 25 (2015).
8. K. An, Ch. An, Ch. Yang, Y. Qing, Y. Shang, Ch. Liu, *Int. J. Electrochem. Sci.*, **12**, 2102 (2017).
9. G. N. Bhar, N. C. Debnath, S. Roy, *Surf. and Coat. Tech.*, **35** (1-2), 171 (1988).

10. W. P. Kripps, in: *Metals Handbook*, ASM, Ohio, 13, 9th edn., 1978, p. 380.
11. Fachikov L., D. Ivanova, D. Dimov, *J. UCTM, Sofia*, **41** (1), 15 (2006).
12. N. A. Perekhrest, K. N. Pimenova, V. D. Litovchenko, L. I. Biryuk, *Zashchita Metallov*, **28** (1), 134 (1992), (in Russian).
13. T. Sugama, T. Takahashi, *J. Mater. Sci.*, **30** (3), 809 (1995).
14. D. Ivanova, L. Fachikov, *Bulg. Chem. Commun.*, **43** (1), 54 (2011).
15. Ts. Dobrev, M. Monev, I. Krastev, W. Richtering, R. Zlatev, St. Rashkov, *Trans. IMF*, **74** (2), 45 (1996).
16. Ts. Dobrev, M. Monev, I. Krastev, R. Zlatev, St. Rashkov, Bulgarian Patent, Registration № 99469, 1995.
17. T. S. N. Sankara Narayanan, *Rev. Adv. Mater. Sci.*, **9**, 130 (2005).